Korean J. Chem. Eng., 35(3), 757-763 (2018)
DOI: 10.1007/s11814-017-0322-8

pISSN: 0256-1115
eISSN: 1975-7220

High selectivity and removal efficiency of lotus root-based activated carbon towards Fe(III) in La(III) solution

Rui-Yan Wu, Yong Wang, Xiao-Yan Xue, Fu-Qiang An†, Tuo-Ping Hu, and Jian-Feng Gao

Chemical Department, North University of China, Taiyuan 030051, Shanxi, P. R. China
(*Received 29 September 2017 • accepted 20 November 2017*)

Abstract−Rare earth elements are an important strategic resource. However, a trace of Fe(III) impurity has serious adverse impact on the performance of rare earth materials. We synthesized a novel nitrogen-containing carbon material, $AC_{LR\text{-}400}$, using lotus root as raw materials. The $AC_{LR\text{-}400}$ was characterized by surface area analyzer, elemental analysis and FT-IR. The selectivity and removal efficiency of $AC_{LR\text{-}400}$ towards Fe(III) were also investigated. The BET specific surface area of $AC_{LR\text{-}400}$ was 68.44 $m^2 \cdot g^{-1}$, and the average pore diameter was 12.54 nm. With abundant nitrogen-containing functional groups and well-developed internal pore structure, $AC_{LR\text{-}400}$ possesses strong adsorption affinity, excellent selectivity and removal efficiency for Fe(III). The adsorption capacity of $AC_{LR\text{-}400}$ towards Fe(III) could reach to 0.46 mmol·g^{-1}, selectivity coefficient with respect to La(III) was 8.9, and removal efficiency was 99.61%. The adsorption isotherm data greatly obey the Freundlich isotherm. In addition, $AC_{LR\text{-}400}$ can be regenerated easily and possesses better regeneration ability and reusability.

Keywords: Activated Carbon, Selectivity, Removal Efficiency, Fe(III), Lotus Root

INTRODUCTION

As a typical metallic element, rare earth elements play an important role in our life. Lanthanum, the most important members of the rare earth elements, possesses active chemical activity and abundant reserves, which makes it widely used in traditional industries, such as metallurgy, petroleum, glass, pottery and porcelain, agriculture, textile and leather [1-4]. However, the non-rare earth impurities can seriously damage the performance of rare earth. Efficiently removing these non-rare earth impurities is extremely significant and received an increasing interest along with the development and reform of industrial technology [5,6]. Numerous studies have been carried out in the last century. Current methods of removal impurity ions from rare earth include adsorption, electrochemical process, membrane separation, chemical precipitation method and solvent extraction [7-12]. But some of them have many flaws [13]. For example, electrochemical and chemical precipitation method is expensive and the energy consumption is high. The service life of membrane is short and this leads to the high operating cost. The solvent extraction method easily causes secondary pollutants [14]. However, adsorption method is simple and cheap, desorption rate is fast, the reusability of absorbent is strong. Therefore, it becomes the first choice for removal of impurities [15]. There are many kinds of adsorbents, such as activated carbon, molecular sieve, resin, loess and fly ash [16,17]. Relying on the developed pore structure, large specific surface area, excellent adsorption performance, high chemical stability, and easy regeneration, porous activated carbon becomes a hot spot of current research adsorbent [18-22].

The raw materials of activated carbon mainly include agricultural wastes, wood wastes, mineral materials, etc. Among them, some precursors, such as oil and coal, are non-renewable resources. Compared with them, agricultural wastes and industrial by-products, such as switchgrass, fruit shell, rice straw, plant seed and stalk [23-26], corn straw, are not only low cost, vast sources, and more environmental friendly, but also many of them have high N content which is advantageous to synthesis containing N carbon materials which possess higher adsorption properties than traditional activated carbon [27,28]. In previous study, another activated carbon ($AC_{UF}700$) was prepared using homemade urea formaldehyde resin as raw material and its adsorption and recognition properties towards Fe(III) were studied [5]. However, the yield of urea formaldehyde resin was low, the high carbonization temperature (700 °C) resulted in high energy consumption, and the adsorption capacity (0.23 mmol·g^{-1}) of $AC_{UF}700$ towards Fe(III) was low. So, more affordable and high-performance adsorption materials are very necessary.

Lotus root is abundant and widely distributed in China. It can be used as raw material to easily prepare activated carbon because of its developed pore structure, high content of nitrogen and low carbonization temperature (400 °C) like hemp [29] and ulva fasciata [30]. In this study, the nitrogen-containing porous activated carbon $AC_{LR\text{-}400}$ was synthesized at 400 °C using lotus root as raw materials, The $AC_{LR\text{-}400}$ was characterized by surface area analyzer, elemental analysis and FT-IR. Based on the characterization of pore structure and surface properties, the selectivity, removal efficiency, dynamics and isotherms of $AC_{LR\text{-}400}$ towards Fe(III) in La(III) were investigated. Simultaneously, the recognition mechanism was also

†To whom correspondence should be addressed.
E-mail: anfuqiang@nuc.edu.cn

analyzed.

EXPERIMENTAL

1. Material

Lotus root materials were obtained from a supermarket in the North University of China. All other reagents were purchased from Beijing Chemical Plant (Beijing, China, AR grade).

2. Preparation of AC_{LR-400}

For preparing AC_{LR-400}, lotus root was smashed and washed with distilled water to remove impurities, and then dried at 110 °C for 24 h. Then 20 g of lotus root was mixed with 60 g of KOH in a beaker. The mixture was heated to 300 °C for 2 h and then carbonized at 400 °C for 2 h with heating rate was 2 °C·min^{-1}. Finally, the resultant samples (AC_{LR-400}) were washed to neutral use distilled water, and then dried at 100 °C.

3. Characterizations

The N_2 adsorption-desorption curves were measured using a surface area analyzer (Beijing JWGB BF-JW132F) by nitrogen adsorption at −180 °C using the BET method. Before being measured, the sample was degassed under vacuum at 220 °C for 2 h. Fourier transform infrared (FTIR) spectra of the sample were measured on a Nicolet FT-IR 4800s (Shimadzu, Japan) spectrometer using the traditional KBr pellet technique. The element content was appraised using Vario EL elemental analyzer (Elementar, Germany) The X-ray photoelectron spectroscopy (XPS) was measured with an ESCALAB 250 (Thermo Electron).

4. Batch Adsorption Experiments of Activated Carbon Towards Fe(III)

4-1. Adsorption Experiments

About 0.01 g of AC_{LR-400} was introduced into a conical flask directly. 20 mL of Fe(III) aqueous solution with initial concentration (C_0) of 1.78 mmol·L^{-1} and pH of 2.5 was then added into the conical flask. The conical flask was placed in a shaker at a preset temperature. At different times, the adsorbent was separated using the filter method from the solution and the concentrations (C_t) of Fe(III) solution were determined by inductive coupled plasma emission spectrometer. The adsorption capacity (Q, mmol·g^{-1}) was calculated according to Eq. (1). In the study, the effects of adsorption time, initial concentration, pH, and the dosage of adsorbent on adsorption capacity and ion removal efficiency (R_{eff}) were investigated, respectively.

$$Q = \frac{V(C_0 - C_t)}{m} \quad (1)$$

$$R_{eff} = \frac{C_0 - C_e}{C_0} \times 100\% \quad (2)$$

where C_0 and C_t are the concentration of metal ions at start and t time in the solution (mmol·L^{-1}); V is the volume of the solution (L); m is the weight of absorbent carbon material (g).

4-2. Competitive Adsorption Experiment

To investigate the selectivity and removal efficiency of activated carbon towards Fe(III), a series of binary mixed solution of Fe(III)/La(III) was prepared and batch adsorption was performed to evaluate the selective property by using distribution coefficient (K_d) and selectivity coefficient (k), which can be calculated according to Eq. (3) and Eq. (4).

$$K_d = \left(\frac{C_0 - C_e}{C_e}\right) \times \frac{V/[V]}{m/[m]} = \frac{Q_e/[Q]}{C_e/[C]} \quad (3)$$

$$k = \frac{K_d(Fe)}{K_d(La)} \quad (4)$$

4-3. Repeated use Experiment

Reusability is a critical measurable indicator to evaluate the practical application properties of adsorbent materials. Desorption of adsorbed Fe(III) from sample was also carried out using hydrochloric acid (2 mol·L^{-1}) as eluent at 25 °C. To test the reusability of AC_{LR-400}, the adsorption-desorption procedure was repeated ten times.

RESULTS AND DISCUSSION

1. Characterization

Fig. 1 shows the Fourier transformed infrared (FTIR) spectra of AC_{LR} prepared at different temperature.

FTIR was used to observe the structural characteristics of the obtained sample. For materials, the absorbance peaks at 3,446, 1,400-1,500 cm^{-1} are ascribed to -OH and C=O stretching vibrations, respectively. Obviously, compared to other samples, the C=O vibration peak is stronger in AC_{LR-400}, suggesting the carboxylic group is richer. It also can be seen that the band between 1,500 and 1,650 cm^{-1} is attributed to N-H stretching vibrations. These indicate that activated carbon still retains a certain amount of functional groups, such as hydroxy, carbonyl and amine groups after carbonization. These groups are expected to be the active sites for metal cations. This also can be confirmed from elemental analysis in Table 1.

The N_2 adsorption-desorption isotherms and pore size distribution curve are shown in Fig. 2. The pore properties of AC_{LR-400} are listed in Table 1.

The N_2 adsorption-desorption curves present characteristics of activated carbons. As for AC_{LR-700}, it is obvious that this gives a steep

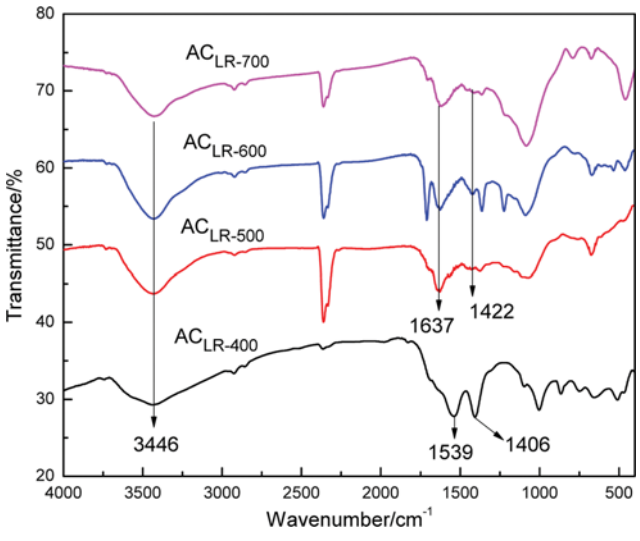

Fig. 1. FTIR spectra.

Table 1. The elemental analysis and pore properties of AC_{LR-400}

Elemental analysis (W_t%)			Structure parameter		
C	N	H	S_{BET} ($m^2 \cdot g^{-1}$)	Pore size (nm)	V_{total} ($cm^3 \cdot g^{-1}$)
43.18	1.65	1.21	68.44	12.54	0.215

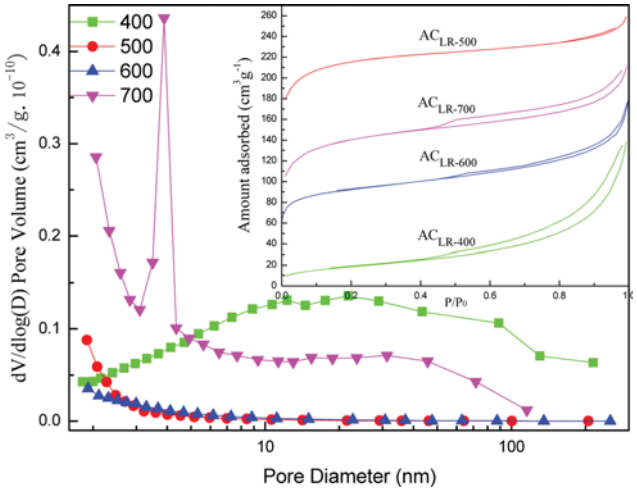

Fig. 2. N_2 adsorption-desorption curves and pore size distribution curve.

type I isotherm with a small hysteresis loop of type H_4 [31,32]. The adsorption and desorption curves were almost overlapped. This indicates that a large amount of micropores with a highly narrow pore size distribution were developed in AC_{LR-700}. As for AC_{LR-400}, the curve is basically type II isotherm. Covered with mesoporous, the pore size distribution in AC_{LR-400} is wider. These also can be obtained from pore size distribution curves in Fig. 2.

2. Kinetic Adsorption

The kinetic adsorption curves of AC_{LR-400} towards Fe(III) and La(III) are shown in Fig. 3.

The adsorption of AC_{LR-400} towards Fe(III) and La(III) reached equilibrium in 8 h and 4 h and the saturated adsorption capacity was 0.46 $mmol \cdot g^{-1}$ and 0.05 $mmol \cdot g^{-1}$, respectively. The AC_{LR-400} showed a better adsorption behavior for Fe(III) than La(III).

To understand the controlling mechanism of the adsorption process, pseudo-first-order [33], pseudo-second-order [34] and intra-particle diffusion models were applied for the experimental data to examine the sorption kinetics. The results are listed in Table 2.

The pseudo-first-order equation is one general equation to describe the adsorption process:

$$\mathrm{Ln}(Q_e - Q_t) = \ln Q_e - k_1 t \quad (5)$$

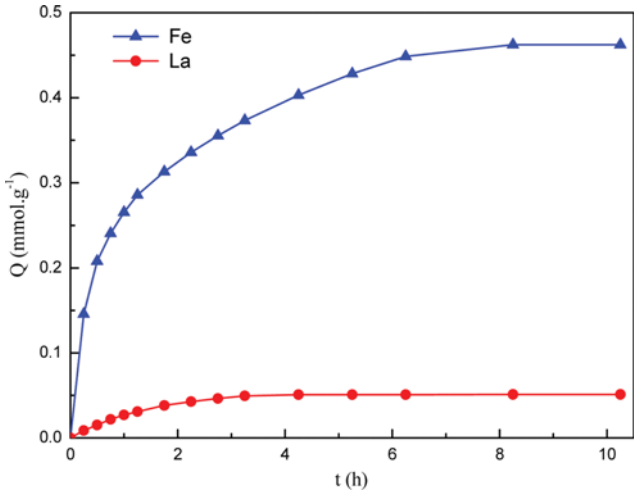

Fig. 3. Adsorption kinetic curves of AC_{LR-400} towards Fe(III) and La(III). pH=2.5, T=25 °C, C_0=1.78 $mmol \cdot L^{-1}$ for Fe(III) and 0.72 $mmol \cdot L^{-1}$ for La(III), dosage=0.5 $g \cdot L^{-1}$.

The pseudo-second-order model is more appropriate to describe the adsorption kinetic behavior in which chemical sorption is the rate-controlling step. The adsorption equation can be expressed as follows:

$$t/Q_t = 1/(k_2 Q_e^2) + t/Q_e \quad (6)$$

To illuminate the diffusion mechanism of adsorption kinetic, intra-particle diffusion model was applied and its equation can be expressed as follows:

$$Q_t = k_{id} t^{1/2} + C \quad (7)$$

where Q_e and Q_t ($mmol \cdot g^{-1}$) are the equilibrium adsorption capacity and adsorption capacity at t time, respectively; k_1 (min^{-1}), k_2 ($g \cdot mol^{-1} \cdot min^{-1}$), and k_{id} ($mmol \cdot g^{-1} \cdot min^{1/2}$) are the rate constant of pseudo-first-order, pseudo-second-order and intra-particle diffusion models; C ($mmol \cdot g^{-1}$) is a constant related to the thickness of the boundary layer.

The values of R^2 for the second-order kinetic model were greater than 0.99, and the calculated equilibrium adsorption capacity was almost close to the experiment data. These indicate that the adsorption of the AC_{LR-400} towards Fe(III) and La(III) were well fit with the second-order kinetic model, and the adsorption mainly depends on the concentration of absorbents and the metal ions, and the adsorption process was a chemical adsorption.

3. Adsorption Isotherm

The adsorption isotherms of AC_{LR-400} towards Fe(III) and La(III) are presented in Fig. 4.

It is evident that the adsorption capacity increases with the ini-

Table 2. Kinetic parameters and correlation coefficients of three kinetic equations

	Pseudo-first-order			Pseudo-second-order			Intra-particle diffusion	
	Q_e/($mmol \cdot g^{-1}$)	k_1/(min^{-1})	R^2	Q_e/($mmol \cdot g^{-1}$)	k_2/($g \cdot mmol^{-1} \cdot min^{-1}$)	R^2	k_{id}/($mmol \cdot g^{-1} \cdot min^{1/2}$)	R^2
Fe(III)	0.46	0.654	0.719	0.51	2.13	0.996	0.12	0.926
La(III)	0.03	0.708	0.816	0.06	16.5	0.990	0.02	0.772

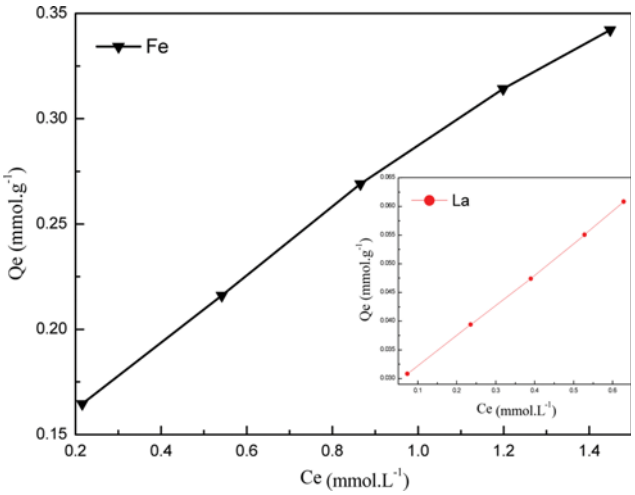

Fig. 4. Adsorption isotherms of AC_{LR-400} towards Fe(III) and La(III). pH=2.5, T=25 °C, dosage=0.5 g·L^{-1}.

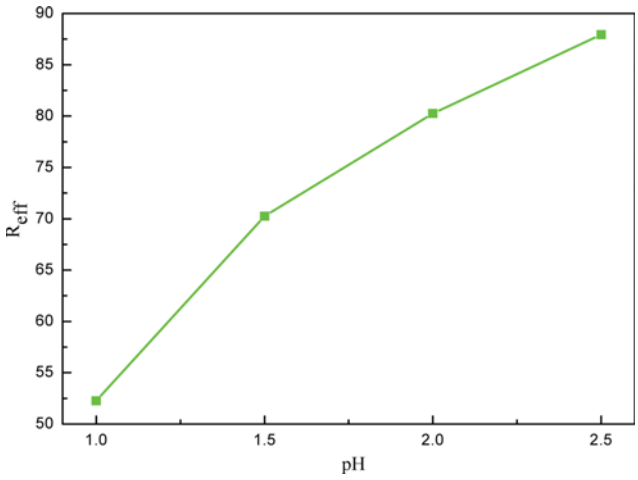

Fig. 5. Effect of solution pH on the removal rate of AC_{LR-400} towards Fe(III). T=25 °C, dosage=5 g·L^{-1}.

tial ion concentration. To further explore the adsorption mechanism, both Langmuir and Freundlich models were applied to interpret the experimental data. The Langmuir model [35] is used successfully to characterize the monolayer adsorption. Whereas the Freundlich isotherm [36] is used commonly to describe the chemical adsorption with a heterogeneous energetic distribution of active sites, along with interaction between adsorbed molecules.

Langmuir equation: $C_e/Q_e=C_e/Q+1/(KQ)$ (8)

Freundlich equation: $LnQ_e=Lnk+(1/n)LnC_e$ (9)

where Q_e (mmol·g^{-1}) is the equilibrium adsorption uptake, Q (mmol·g^{-1}) is the theoretical adsorption capacity of sample for ions, C_e (mol·L^{-1}) is the equilibrium concentration of Fe(III) and La(III), K (L·g^{-1}) is the Langmuir sorption constant relating the free energy of adsorption, and n is the Freundlich parameters related to adsorption uptake and adsorption intensity.

The isotherm constants and correlation coefficient (R^2) are summarized in Table 3. The R^2 values indicate that the Freundlich equation affords a better interpretation of the experimental data than does the Langmuir equation. Thus, the AC_{LR-400} adsorbed ions not only by monomolecular layer, but also through chemical adsorption. These results are consistent with the results of FTIR and kinetic adsorption data. And the applicability of amount of active functional groups such as N-H and C=O coverage on AC_{LR-400} was confirmed.

4. Effect of pH

It is well-known that the pH plays a key role in controlling the process of adsorption. It affects not only the surface charge of the absorbent, but also the degree of ionization in solution. Fig. 5 shows the influence of pH on adsorption capacity of AC_{LR-400} to Fe(III).

Clearly, the pH has an unignorable influence on the Fe(III) removal efficiency, and the removal efficiency of AC_{LR-400} towards Fe(III) increases gradually with the increase of solution pH. The maximum removal efficiency of Fe(III) was 87.7% at pH 2.5. At lower pH, nitrogen atoms of activated carbon were protonated entirely so the active sites were less available for metal ions, and the activated carbon could not effectively interact with the metal ions. With the increase of the solution pH, the protonation degree of N atoms was lowered, which enhanced the coordination interaction. So, the metal ions can be more easily bound on the active centers and the adsorption capacity increases with the increase of the solution pH.

Table 3. Fitting parameters and correlation coefficients of Langmuir and Freundlich

	Langmuir			Freundlich		
	Q (mmol·g^{-1})	K (L·g^{-1})	R^2	k	n	R^2
Fe(III)	0.44	0.039	0.971	3.40	2.58	0.986
La(III)	0.07	0.049	0.959	3.25	2.00	0.977

5. Effect of Dosage

The influence of adsorbent dosage on removal efficiency of AC_{LR-400} towards Fe(III) from pure Fe(III) solution and mixed Fe(III)/La(III) binary mixture is shown in Fig. 6.

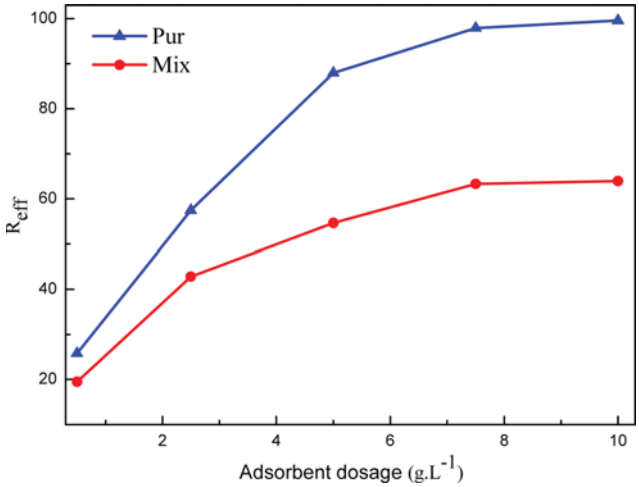

Fig. 6. Removal rate of AC_{LR-400} towards Fe(III) at different condition. T=25 °C, pH=2.5.

Table 4. Distribution coefficient and selectivity coefficient data

pH	Initial concentration ($mmol \cdot L^{-1}$)		K_d ($L \cdot g^{-1}$)		k (Fe/La)
	Fe(III)	La(III)	Fe(III)	La(III)	
2.5	1.78	0.72	0.537	0.060	8.95
2	1.78	0.72	0.215	0.024	8.96

As can be seen, the removal efficiency increases gradually with increase of adsorbent dosage and becomes almost constant at adsorbent dosage of 7.8 $g \cdot L^{-1}$. This can be explained by the increase of more binding sites and making easier penetration of metal ions to the adsorption sites.

The removal efficiency of AC_{LR-400} to Fe(III) from pure Fe(III) solution was better than from mixture; the reason was that the binding site of activated carbon was limited, and a competitive adsorption exists between Fe(III) and La(III).

6. Adsorption Selectivity

The competitive adsorption of AC_{LR-400} towards Fe(III) in Fe(III)/La(III) mixtures was researched by batch method. Table 4 summarizes the data of the distribution coefficients and selectivity coefficients.

In Table 4, AC_{LR-400} has high selectivity for Fe(III), and the selective coefficient can reach 8.95 at pH of 2.5. This is attributed to the special electronic structure of La(III), which makes coordinating ability of La(III) with N atoms weaker, while that of Fe(III) with N atoms is stronger. So, the N atoms only coordinate with Fe(III) and do not coordinate with La(III) when Fe(III) and La(III) exist simultaneously. According to this analysis, AC_{LR-400} could selectively remove Fe(III) from Fe(III)/La(III) mixture solution, and AC_{LR-400} has excellent recognition selectivity towards Fe(III).

To analyze the adsorption and recognition selectivity mechanism, XPS method was further used to study the surface chemical compositions of AC_{LR-400}, Fe, and La. The XPS of AC_{LR-400} and metal ion-loaded AC_{LR-400} were determined, and the detailed deconvolution results are listed in Table 5.

The signal of metal ion is observed in the spectra of metal ion-loaded AC_{LR-400}, and this attests to the adsorption of AC_{LR-400} towards metal ions.

Some important laws can be also found from Table 3. First, the binding energy of C and O has almost no change, and this indicates that C and O did not coordinate with metal ions despite carboxylic groups being able to interact with metal ions. Secondly, a new signal of N, Fe, and La was observed in the spectra of single metal ion-loaded AC_{LR-400} (AC_{LR-400}-Fe and AC_{LR-400}-La). The binding energy of N increases and that of Fe and La decreases. These indicate that coordination bonds (N→Fe, N→La) are formed between the lone pair electrons of N and unoccupied orbital metal ions. The outer electrons migration of N makes N having higher valence state, so the binding energy is increased. Lastly, the new signal of N and Fe is also observed in spectra of double metal ion-loaded AC_{LR-400} (AC_{LR-400}-Fe/La), but the new signal of La is not observed. This indicates that the N atoms only coordinate with Fe and not with La when Fe and La exist simultaneously, and this is attributed to the special electronic structure of La. The special electronic structure results in the weaker coordinating ability and larger coordination number, and the La adsorbed by means of coordination could be replaced by Fe with stronger coordinating ability. Based on the above analysis, AC_{LR-400} has excellent recognition selectivity towards Fe(III) and AC_{LR-400} could selectively adsorb Fe(III) from Fe(III)/La(III) mixture solution.

7. The Influence of Concomitant Metal Ion on Adsorption Capacity and Selectivity

There are usually contained several kinds of metal cations in actual rare earth solution including Na(I), K(I), and Ca(II), which

Table 5. XPS analysis

XPS peak		$FeCl_3$	$LaCl_3$	AC_{LR-400}	AC_{LR-400}-Fe	AC_{LR-400}-La	AC_{LR-400}-Fe/La
					704.91		704.92
Fe($2p_{3/2}$)		706.95			706.79		706.74
					718.10		718.35
Fe($2p_{1/2}$)		720.14			720.13		720.10
						834.69	
La($3d_{5/2}$)			836.24			836.02	836.29
						853.79	
			854.97			854.83	854.63
C(1*s*)	C-H			284.32	284.25	284.31	284.26
	C-O			285.21	285.31	285.25	285.28
	C=O			287.43	287.37	287.38	287.42
O(1*s*)	O=C			530.45	530.62	530.52	530.43
	O-H			532.14	532.15	532.21	532.24
	O-C			533.86	533.82	533.83	533.78
N(1*s*)	>N-			398.14	398.12	398.15	398.11
					399.78	399.79	399.76
	-NH-			400.17	400.21	400.19	400.15
					401.34	401.36	401.33

Table 6. The adsorption capacity and selectivity of AC_{LR-400} towards Fe(III) and La(III) under different concomitant ions

Concomitant ions	Concentration ($mmol \cdot L^{-1}$)	Q ($mmol \cdot g^{-1}$)		k (Fe/La)
		Fe(III)	La(III)	
	0.5	0.46	0.05	8.95
Na(I)	1.0	0.46	0.05	8.95
	2.0	0.45	0.04	8.97
	0.5	0.46	0.05	8.95
K(I)	1.0	0.46	0.04	8.96
	2.0	0.45	0.04	8.97
	0.5	0.44	0.04	8.94
Ca(II)	1.0	0.42	0.04	8.91
	2.0	0.40	0.03	9.02

Note: The concentration of Fe(III) and La(III) is 1.78 and 0.72 $mmol \cdot L^{-1}$, respectively; dosage=0.5 $g \cdot L^{-1}$; temperature: 25 °C; adsorption time: 8 h; pH: 2.5

may lead to competitive adsorption against Fe(III) and La(III). The adsorption capacity and selectivity of AC_{LR-400} towards Fe(III) and La(III) under different concentration of concomitant ions (0.5-2.0 $mmol \cdot L^{-1}$) was also investigated using batch method. The results are listed in Table 6.

As can be seen in Table 5, the alkaline metal cation ions (Na(I) and K(I)) have almost no suppressive effect on the adsorption ability and selectivity of AC_{LR-400} towards Fe(III) and La(III), while the adsorption capacity slightly decreases with increasing Ca(II) concentration from 0.5 $mmol \cdot L^{-1}$ to 2.0 $mmol \cdot L^{-1}$. This is likely attributed to AC_{LR-400} possessing stronger complexation ability with heavy metal ions, and this indicates further that AC_{LR-400} could selectively adsorb Fe(III) from La(III) solution under the alkaline and alkaline earth metal ions background.

8. Desorption and Reusability

To demonstrate the repeatability of the AC_{LR-400}, adsorption-desorption cycle towards Fe(III) was carried out ten times by batch method. The result is shown in Fig. 7.

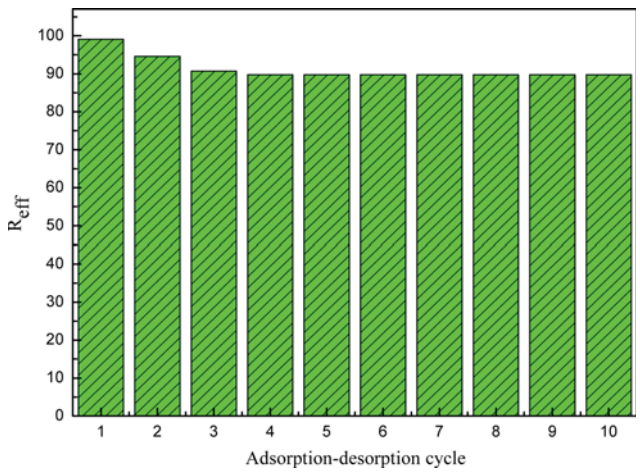

Fig. 7. Adsorption-desorption cycle. T=25 °C, pH=2.5, dosage=8 g·L^{-1}.

The adsorption capacity of AC_{LR-400} decreases slightly in the first four cycles, the removal percentage of Fe(III) was no less than 30% in the four cycles. This may result from the collapse of some hole structure and the disappearance of the functional group. This clearly indicates that the AC_{LR-400} has excellent reusability.

CONCLUSIONS

A nitrogen-containing activated carbon, AC_{LR-400}, was synthesized successfully using lotus root carbonized at 400 °C. The BET specific surface of AC_{LR-400} was 68.44 $m^2 \cdot g^{-1}$, and the average pore size was 12.54 nm. With its well-developed internal pore structure and abundant functional groups, such as C=O and N-H, AC_{LR-400} possesses strong adsorption performance and excellent recognition selectivity for Fe(III) in Fe(III)/La(III) solution. The maximum adsorption amount towards Fe(III) was 0.46 $mol \cdot g^{-1}$. The adsorption process greatly obeys the Freundlich model. The removal efficiency for Fe(III) was almost 100% at 7.8 $g \cdot L^{-1}$. The selectivity coefficient to Fe(III) reaches 8.9. In addition, adsorbed ions can be easily desorbed using diluted hydrochloric acid solution as eluent. AC_{LR-400} is considered to be effective and promising adsorbent for removing Fe(III) from La(III).

ACKNOWLEDGEMENTS

The authors gratefully acknowledge the financial support by the International Science & Technology Cooperation Program of China (No. 2011DFA51980), National Scientific Foundation of China (No. 5110423), Shanxi Science & Technology Cooperation Program of China (No. 2015081043), and Science Foundation of Shanxi Province (No. 20140313002-4, 20130321022-02, 2013021012-3).

REFERENCES

1. F. Q. An, B. J. Gao and X. W. Huang, *React. Funct. Polym.*, **73**, 60 (2013).
2. G. L. Ou, J. F. Gao and T. P. Hu, *RSC Adv.*, **5**, 71878 (2015).
3. C. Tunsu and T. Retegan, *Hydrometallurgy*, **6**, 139 (2016).
4. Y. Y. Wang, H. H. Lu and Y. X. Liu, *Colloids Surf., A.*, **509**, 550 (2016).
5. F. Q. An, R. Y. Wu and M. Li, *Environ. Chem. Eng.*, **5**, 1638 (2017).
6. W. S. Wang, Y. B. Li and B. J. Gao, *Eng. Res. Des.*, **91**, 2759 (2013).
7. W. J. Peng, H. Q. Li and Y. Y. Liu, *J. Mol. Liq.*, **230**, 496 (2017).
8. F. N. Behdani and A. T. Rafsanjani, *Korean J. Chem. Eng.*, **30**, 448 (2013).
9. S. B. Khan, H. M. Marwani and J. Seo, *Bull. Mater. Sci.*, **38**, 327 (2015).
10. N. Sui, K. Huang and J. Y. Lin, *Sep. Purif. Technol.*, **127**, 97 (2014).
11. M. M. Rahman, S. B. Khan and H. M. Marwani, *J. Taiwan Inst. Chem. E.*, **45**, 1964 (2014).
12. M. R. Karim, H. Takehira and M. M. Rahman, *J. Organomet. Chem.*, **808**, 42 (2016).
13. P. D. Saha, S. Chowdhury and S. Datta, *Korean J. Chem. Eng.*, **29**, 1086 (2012).
14. B. J. Gao, J. Y. Meng and Y. Xu, *J. Ind. Eng. Chem.*, **24**, 351 (2015).
15. C. M. Parka, J. Hanb and K. H. Chu, *J. Ind. Eng. Chem.*, **48**, 186 (2017).

16. K. S. Ryoo, S. Y. Jung and H. Sim, *Bull. Korean Chem. Soc.*, **34**, 2753 (2013).
17. B. Li, L. Yang and C. Q. Wang, *Chemosphere*, **175**, 332 (2017).
18. X. Han, H. F. Lin and Y. Zheng, *J. Hazard. Mater.*, **297**, 217 (2015).
19. X. C. Lu, J. C. Jiang and K. Sun, *Bull. Korean Chem. Soc.*, **35**, 103 (2014).
20. Y. Zhou, O. G. Apul and T. Karanfil, *Water Res.*, **79**, 57 (2015).
21. Z. G. Zhang, X. Q. Feng and X. X. Yue, *Korean J. Chem. Eng.*, **32**, 1564 (2015).
22. S. Bhati, J. S. Mahur and S. Dixit, *Bull. Korean Chem. Soc.*, **34**, 569 (2013).
23. M. Essandoh, D. Wolgemuth and C. U. Pittman Jr., *Chemosphere*, **174**, 49 (2017).
24. Z. X. Tan, Y. H. Wang and A. Kasiuliene, *Clean Technol. Environ. Policy.*, **19**, 761 (2017).
25. Z. M. Zou, Y. L. Tang and C. H. Jiang, *J. Environ. Chem. Eng.*, **3**, 898 (2015).
26. B. Li, L. Yang and C. Q. Wang, *Chemosphere*, **175**, 332 (2017).
27. Y. S. Yun, D. Kim and H. H. Park, *Synth. Met.*, **162**, 2337 (2012).
28. J. H. Kim, S. Cho and T. S. Bae, *Sens. Actuat. B.*, **197**, 20 (2014).
29. M. R. Juana, B. Jorge and R. M. José, *Ind. Eng. Chem. Res.*, **47**, 1288 (2008).
30. J. R. P. Suresh and V. Chandrasekaran, *Pol. J. Chem. Tech.*, **14**, 88 (2012).
31. J. Rouquerol, D. Avnir and C. W. Fairbridge, *Pure Appl. Chem.*, **66**, 1739 (1994).
32. M. Thommes, R. Guillet-Nicolas and K. A. Cychosz, Wiley-VCH Verlag GmbH & Co. KGaA, Weinheim, 349 (2015).
33. S. Lagergren, K. Svenska Vetensk Akad. Handl., **24**, 1 (1898).
34. Y. S. Ho and G. McKay, *Process Biochem.*, **34**, 451 (1999).
35. I. Langmuir, *J. Am. Chem. Soc.*, **38**, 2221 (1916).
36. H. M. F. Freundlich, *Z. Phys. Chem.*, **57**, 385 (1906).